Provided for non-commercial research and educational use only.
Not for reproduction or distribution or commercial use.

Volume 84, Issues 5-8 May/August 2007 ISSN 0167-9317

MICROELECTRONIC ENGINEERING

An International Journal of Semiconductor Manufacturing Technology

Including Nanoelectronic Engineering

www.elsevier.com/locate/mee

MICRO and NANOENGINEERING

MNE2006

Proceedings of the 32nd International Conference on Micro- and Nano-Engineering

17 – 20 September 2006
Barcelona, Spain

Edited by:
Joan Bausells
Gabriel Abadal and
Francesc Pérez-Murano

This article was originally published in a journal published by Elsevier, and the attached copy is provided by Elsevier for the author's benefit and for the benefit of the author's institution, for non-commercial research and educational use including without limitation use in instruction at your institution, sending it to specific colleagues that you know, and providing a copy to your institution's administrator.

All other uses, reproduction and distribution, including without limitation commercial reprints, selling or licensing copies or access, or posting on open internet sites, your personal or institution's website or repository, are prohibited. For exceptions, permission may be sought for such use through Elsevier's permissions site at:

http://www.elsevier.com/locate/permissionusematerial

ELSEVIER

Available online at www.sciencedirect.com

Microelectronic Engineering 84 (2007) 1446–1449

MICROELECTRONIC ENGINEERING

www.elsevier.com/locate/mee

Design and fabrication of high-efficiency fibre couplers for nanophotonic devices

D.M. Beggs [a,*], M. Ayre [a], D.F.G. Gallagher [b], T.F. Krauss [a]

[a] School of Physics and Astronomy, University of St Andrews, North Haugh, St Andrews KY16 9SS, UK
[b] Photon Design, 34 Leopold Street, Oxford OX4 1TW, UK

Available online 30 January 2007

Author's personal copy

Abstract

A dual waveguide heterostructure device that couples light from single mode optical fibres into nanophotonic devices with an overall modelled efficiency of 81% has been investigated. A four-stage taper design for the ridge waveguide which allows for a total device length of 610 μm is described. The fabrication of the ridge waveguide using chemically-assisted ion-beam etching has been optimised.
© 2007 Elsevier B.V. All rights reserved.

Keywords: CAIBE; Etching; Indium phosphide; Tapers; Waveguides

1. Introduction

There are three main aspects of the realisation of photonic crystal-based devices for miniaturised semiconductor optoelectronic devices. These are active functions, passive functions and active–passive integration. The indium phosphide (InP) material system provides promising scope for the realisation of all three, given the availability of gain in the near IR wavelength window. Given that the material properties can be engineered in a wide range, passive functions, e.g. for spectral selection and polarisation diversity, can be realised equally well, and monolithically. This paper focuses on efforts to design and fabricate a passive device that will efficiently couple light from optical fibres into and out of nanophotonic devices in the InP material system. Direct coupling from standard fibres to nanophotonic devices is inefficient, owing to the large refractive index contrast, geometric size differences and the profile of the optical modes. For example, the cross-section of the mode of a single mode fibre is ~65 μm^2, while at the other extreme, that of a photonic crystal waveguide [1] can be as small as 0.1 μm^2. Thus, 20–30 dB coupling loss can be expected if the two are simply butt-coupled together.

Various schemes that employ nano-tapers have been proposed and investigated in other material systems [2–8]. For example, in the silicon-on-insulator system, polymer overlayers with inverse tapers have been used [2], but this scheme is not available for the InP material system due to the large refractive index of InP-based layers. However, a similar inverse taper design, based on a dual waveguide heterostructure with a buried waveguide and a tapered ridge waveguide, can be realised, as illustrated in Fig. 1. The buried waveguide layers are designed to give an optical mode that is well matched to the circular mode of a single mode optical fibre. The tapering of the ridge waveguide then adiabatically matches the mode of the ridge waveguide to that of the buried waveguide, in order to induce vertical coupling. Fig. 2 shows the calculated intensity of the modes of the structure for ridge waveguides of widths 0.5, 0.6, 0.7, 0.8 and 0.9 μm, and this illustrates the intended principle of operation for the coupler. The modelling was performed for a wavelength of 1.55 μm.

The efficiency of the coupling from the buried waveguide to the ridge waveguide has been investigated, and, for a linear taper, a device length of 3 mm is required before this efficiency reaches 95%. Therefore, in order that on-chip

* Corresponding author. Tel.: +44 1334 46733.
E-mail address: daryl.beggs@st-andrews.ac.uk (D.M. Beggs).

0167-9317/$ - see front matter © 2007 Elsevier B.V. All rights reserved.
doi:10.1016/j.mee.2007.01.073

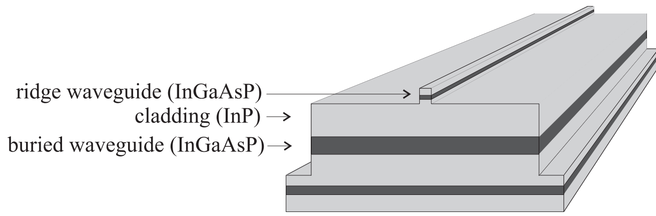

Fig. 1. Schematic illustration of the proposed dual heterostructure device. The dark regions are the quaternary InGaAsP waveguide layers, and the light regions are the InP cladding layers.

designs remain compact, a four-stage taper, where the angle of each stage is allowed to vary, has been designed. Using such a scheme, nearly 100% transmission from the buried waveguide into the ridge waveguide can be achieved for a total device length of 610 μm. Fig. 3 shows the angle of the taper against the width of the ridge waveguide for the four-stage design. For comparison, a 3 mm long linear

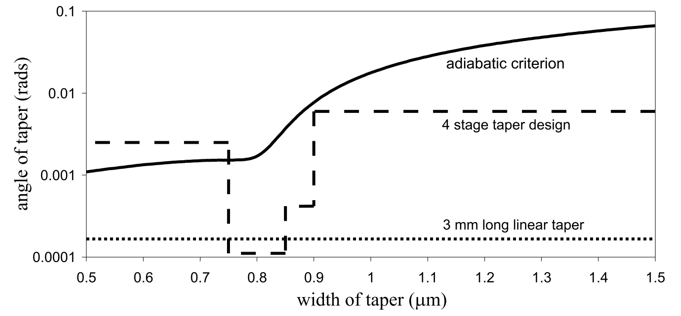

Fig. 3. Angle of the tapered ridge waveguide against its width for the four-stage design (dashed line). A 3 mm linear taper (dotted line) and the adiabatic criterion (solid line) are also shown.

taper and the criterion for adiabatic coupling are also shown. The first (narrowest) stage has a relatively large angle which breaks the adiabatic criterion, but as the

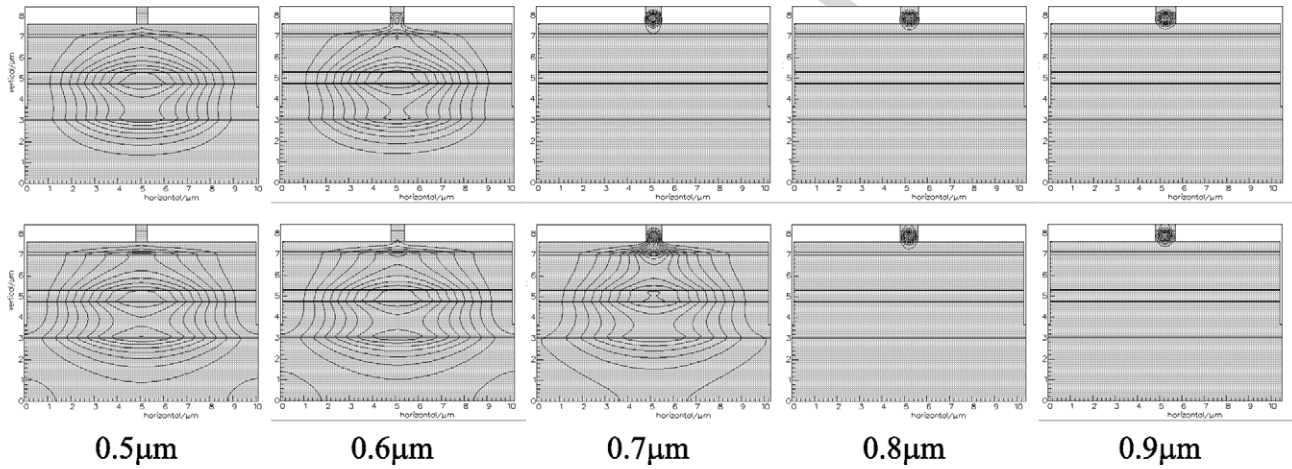

Fig. 2. Calculated intensity of modes of the double heterostructure for ridge waveguides of the indicated width. The top sequence shows TM-polarised modes, and the bottom shows TE-polarised modes.

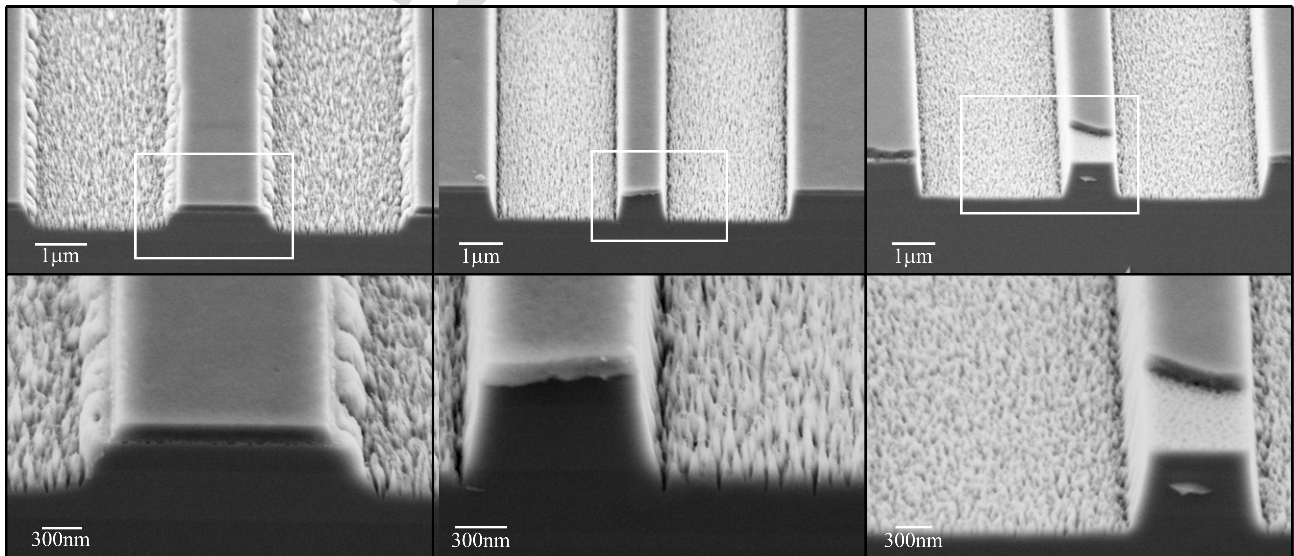

Fig. 4. The effect of temperature on the CAIBE etching of the ridge waveguide. From left to right the temperature of the etch is 170, 200 and 230 °C. The bottom images show the detail of the trench floor and side walls, as indicated by the white boxes in the top images.

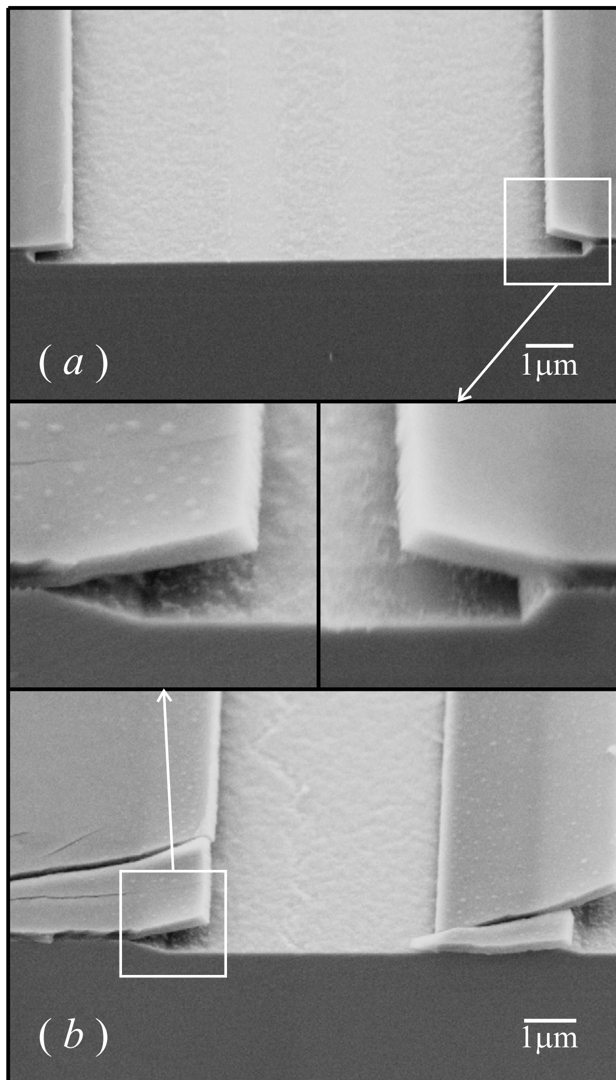

Fig. 5. The effect of wet etching for 1 min with a 50:50 solution of hydrochloric:phosphoric acid. There are large undercuts in of the mask, and two perpendicular directions of the trenches on the InP wafer give straight side walls (a) or slanted side walls (b).

majority of the intensity is concentrated in the buried waveguide in this region, the large angle is non-critical to the device performance. The second stage is the critical region where the vertical coupling between the waveguides occurs, and the angle of this stage is small (0.05°). This stage accounts for almost 3/4 of the total device length. The final (widest) stages have larger angles (below the adiabatic criterion) in order to shorten the device length. The overall efficiency of the fibre to nanophotonic device – a W3 photonic crystal waveguide was modelled – has been calculated to be 81% for a single mode optical fibre.

2. Fabrication

The dual waveguide wafers were supplied by Alcatel, and consist of InP layers and InGaAsP waveguide layers. The fabrication of the ridge waveguide requires the accurate etching of the top InP and InGaAsP layers to an accurate depth of around 1 μm, to form trenches either side of the ridge. The trenches are first defined using electron beam lithography in PMMA resist (950 K molecular weight, 300 nm thick), which is then used to transfer the pattern to a flowable oxide (deposited by spin coating) hard mask using reactive ion etching with CHF_3 chemistry. The lithography is challenging, as the angle of the four stages must be accurately controlled to within 0.05°. Due to the area of the trenches required for the tapers, the step size of the electron beam writer must be kept relatively large (~30 nm) in order that the writing time is kept reasonable. The staircase approximation that the electron beam writer uses for the angled tapers can result in unacceptable back-scattering in the final etched device. Thus the pattern is over-exposed by 10–20% in order to smooth out the staircase. The etching of the InP layers is then achieved using chemically-assisted ion-beam etching (CAIBE). The conditions for the deep etching of InP using CAIBE have been previously investigated [9], and smooth sidewalls can be obtained. However, these etch conditions result in a rough etch floor, which would hamper device performance by causing scattering losses. The rough etch floor is a result of "grass" caused by the etching, and the resettling of reaction products during the etch. Therefore, the CAIBE conditions have been modified to produce smoother etch floors whilst retaining the straight side walls. The temperature, gas flow and ion-beam parameters have been independently varied in order to optimise the process. For example, Fig. 4 shows the effect of temperature on the resultant etching. Increasing the temperature leads to an increase in the etch rate and also a decrease in the size of the grass on the trench floor. This is due to the promotion of the chemical reaction between the Cl_2 gas and the InP layers and the increase of the mobility of the reaction products at higher temperatures. Another notable parameter is the gas flow rate – by decreasing this rate, the partial pressure in the etched trenches is lowered, which promotes the escape of the reaction products from the trench before resettling occurs. The optimised etch conditions are a temperature of 230 °C, a Cl_2 gas flow rate of 5 sccm, an Ar gas flow rate of 5 sccm, a beam voltage of 350 V and a beam current of 10.0 mA, and the result of this etch is shown in Fig. 4 (right images).

We have also investigated the possibility of wet etching the trenches. However, standard etches based on hydrochloric/phosphoric acids are selective (they do not etch the quaternary InGaAsP waveguiding layer) and result in large undercuts of the hard mask, as shown in Fig. 5. Also, the trenches have to be orientated correctly to the InP crystal [10], in order to etch the correct crystal face and achieve straight sidewalls (Fig. 5a). If these conditions were met, we still observe that the parallel orientation results in slanted side walls (Fig. 5b). We therefore conclude that wet etching is not suitable for creating the ridges, also given the tight

Author personal copy

size tolerances, although a short wet etch may be used as a post dry-etch step, in order to improve the smoothness of the etch floor.

In summary, the design and fabrication of a fibre coupler for nanophotonic devices has been investigated for the InP material system. A dual heterostructure with buried and ridge waveguides is used, and a four-stage taper design that adiabatically matches the mode of the ridge waveguide to that of the buried waveguide is presented. The optimal CAIBE etch conditions that provide almost smooth floors and straight side walls in the fabrication of the ridge waveguide are given.

Acknowledgement

We wish to acknowledge the support of the EU-IST "Funfox" STREP project.

References

[1] T.F. Kruass, Photonic Crystals Shine On, Physics World, 2006.
[2] S.J. McNab, N. Moll, Y.A. Vlasov, Opt. Exp. 11 (22) (2003) 2927–2939.
[3] V.R. Almeida, R.R. Panepucci, M. Lipson, Opt. Lett. 28 (15) (2003) 1302–1304.
[4] Y. Shani, C.H. Henry, R.C. Kistler, K.J. Orlowsky, D.A. Ackerman, Appl. Phys. Lett 55 (23) (1989) 2389–2391.
[5] M. Lipson, Nanotechnology 15 (2004) S622–S627.
[6] W. Bogaerts, D. Taillaert, B. Luyssaert, P. Dumon, J. Van Campenhout, P. Bienstman, D. Van Thourhout, R. Baets, V. Wiaux, S. Beckx, Opt. Exp. 12 (8) (2004) 1583–1591.
[7] D. Taillaert, F. Van Laere, M. Ayre, W. Bogaerts, D. Van Thourhout, P. Bienstman, R. Baets, Jpn. J. Appl. Phys. Part 1 45 (8A) (2006) 6071–6077.
[8] F. Van Laere, M. Ayre, D. Taillaert, D. Van Thourhout, T.F. Krauss, R. Baets, Electron. Lett. 42 (6) (2006) 343–345.
[9] M.V. Kotlyar, L. O'Faolain, R. Wilson, T.F. Krauss, J. Vac. Sci. Technol. B 22 (4) (2004) 1788–1791.
[10] S.E.H. Turley, P.D. Greene, J. Cryst. Growth 58 (1982) 409–416.

Author's personal copy